Mawer *et al. Animal Biotelemetry* (2026) 14:14
https://doi.org/10.1186/s40317-026-00453-5

Animal Biotelemetry

RESEARCH Open Access

Going with the flow: tidal and tag influences upon the performance of acoustic telemetry systems

Rachel Mawer[1*], Novella Franconi[1], Toby Linley-Adams[1], Georgie Blow[1], Oliver Duke[1], Amelia Jones[1], Carina Rees[1], Mark Breckels[2], Stephen Gregory[3,4], David Maxwell[2], Randolph Velterop[5] and David Clarke[1]

Abstract

Background Acoustic telemetry is a widely used tool for studying the behaviour of aquatic species. Underpinning acoustic telemetry research is an understanding of parameters influencing the ability of receivers to detect tags, facilitating accurate study design and interpretation of the data. Tide is a regular predictable phenomenon that may affect detection probabilities, for example via signal loss and/or distortion due to water movement. Here, we examined the performance of acoustic receivers in the Bristol Channel, UK (an area with one of the largest tidal ranges in the world), investigating the influence of tidal phase, tidal height and other covariates such as receiver orientation and depth on the detection efficiency of acoustic tags.

Results Tidal phase had a strong influence on detection efficiency, with reduced detection efficiency during the mid-tide period when water movement was greatest. Detection efficiency was further reduced during spring tides, where tidal flow is increased, and with larger surface waves. Moreover, surface-deployed receivers experienced stronger tidal effects compared to receivers deployed on the seabed. Detection range varied with tide, falling during mid-tide periods. The distance at which 50% of expected pings were detected fell by 44% for low power test tags from high water to mid-tide. Detection ranges also varied with tag model and power, with low-power tags having smaller detection ranges compared to high power, and test tags having smaller detection ranges compared to receiver sync tags.

Conclusions Detection efficiency and range can strongly vary throughout the tidal cycle. Neglecting the tidal cycle when analysing acoustic telemetry data may result in erroneous conclusions regarding animal behaviour in response to tide (e.g. incorrectly assuming animal absence is due to tide) or poor study design for future studies (e.g. fine-scale arrays with receiver spacing too wide for positioning during mid-tide periods). Given the regular nature of tide, we highlight the need for acoustic telemetry users to quantify and understand tidal influence on their study systems with the same tag models as to be used by animals and adjust study design and data analysis appropriately.

Keywords Acoustic telemetry, range test, detection range, detection efficiency, tidal effects

*Correspondence:
Rachel Mawer
rachel.mawer@swansea.ac.uk

Full list of author information is available at the end of the article

Graphical abstract

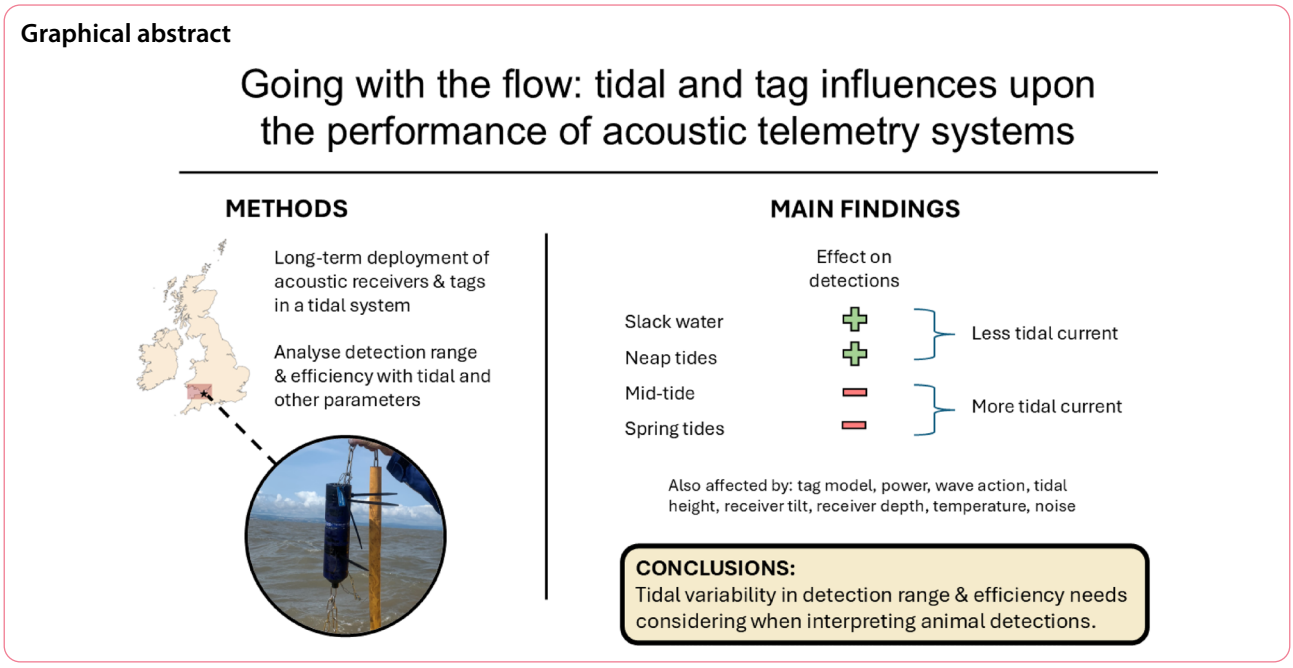

Background

Acoustic telemetry is a widely used tool for studying the movement of aquatic species. Animals are tagged with an acoustic transmitter, or tag, which emits a unique coded signal that is decoded and recorded by underwater hydrophones (acoustic receivers). Acoustic telemetry has been applied across ecosystems, spatio-temporal scales and taxa, targeting species ranging from cephalopods and crustaceans to elasmobranchs and cetaceans [1]. Acoustic telemetry can shed light upon animal movements, from broad-scale movements along continental coasts [2] to precise positions within a discrete area on sub-minute intervals [3]. With advancing technology enabling new tag types such as those which can detect predation events [4] to the development of new methods for analysis and global networks for sharing data which facilitates the identification of transboundary movements [5–7], acoustic telemetry research is proliferating [8].

Detections of tagged animals at receivers can provide insight into a wide array of animal behaviours. Detections at different receivers can provide valuable data on animal movement, while detections in discrete areas can provide measures of residency, giving researchers an insight into spatial usage and drivers [2, 9]. For example, recent work with acoustic telemetry has linked changes in bull shark (*Carcharhinus leucas*) residency and migration timings to warming oceans [10]. Where receivers are deployed with overlapping detection ranges, fine-scale acoustic telemetry can estimate precise positions of animals that are detected by multiple receivers simultaneously, producing precise tracks of animal movements and new insights into animal behaviour, such as behavioural responses to hydraulic cues [11], habitat preferences [3] and social behaviour [12]. However, the ability of a receiver to detect a transmitter is reliant on the propagation of that signal through water, with distance a major limiting factor due to energy loss as the signal moves through the water [13]. Where environmental conditions further limit signal propagation, the detection probability and range – the relationship between distance and detection probability [14] – will be lessened. Consequently, a lack of detections does not necessarily indicate absence, and insights from acoustic telemetry are underpinned by an understanding of system performance and its variability with environmental conditions.

The variability of detection probability has been well described with many parameters, though results can vary with study location. Habitat type, topography, vegetation and bathymetry affect detection range [14–16], for example with greater detection ranges in homogenous habitats [17]. Weather conditions can introduce temporal variability in detection probabilities, with detection probability falling with increasing wind speeds [18, 19] and increasing rain [20] – though not always [18]. Temperature also affects detection probability, via affecting the speed of sound [14], seasonal stratification of the water column [21] and/or thermoclines [22]. Similarly, increased levels of background noise in a system can also reduce detection range, as noise can interrupt or overpower transmitted signals [14, 18, 19, 22]. If detection probability is reduced under certain conditions and researchers neglect to consider this, interpretations may be false: were there fewer animals in the system under these conditions or could we simply not detect them?

Indeed, Payne et al. [23] demonstrated that apparent diel patterns in cuttlefish movement were instead a product of diel variation in detection efficiency rather than animal behaviour. Moreover, understanding of detection ranges and efficiencies is essential in shaping the study design. For example, Radigan et al. [24] modified their receiver array based on detection range analysis to optimise detection distance. Where the intention is to develop a fine-scale array, which is dependent on overlapping receiver detection ranges, knowing that detection range may drop predictably could enable appropriate receiver spacing and data collection across a range of conditions. As such, it is vital to understand how array performance may vary under expected conditions at the study site in question: something often neglected with many studies opting to use detection range figures published in other literature [14].

A key variable affecting acoustic array performance is the tidal cycle. Tide is a regular and predictable phenomenon affecting coastal and estuarine systems, with alternating periods of slack and moving water. Tide could affect detection through multiple mechanisms. In between low and high waters, when tidal currents are present, the water movement may affect receiver performance via signal loss/distortion and/or increased noise: increased water movement causes reduced detections and positions of animals in acoustic telemetry arrays [19, 25–28]. Moreover, water currents may cause receivers to be tilted [28], creating a detection shadow from which direction efficiency is lessened [18]. Tide also introduces changes in water depth, via tidal height, further impacting tag detection. For example, Long et al. [29] reported higher efficiencies as water depth increased for a range of 0–10 m, indicating limited performance in shallower waters. Additionally, increased turbidity and suspended particulate matter in the water column due to tidal flow could interrupt signal propagation, limiting detection probability and range [30]. Given the regular, predictable nature of tide coupled with the fact that tide may influence animal behaviour, it is vital to understand how tide may influence receiver detection efficiency. While variation in detection efficiency with tidal cycle has been described before, there is further research to be done. Bruneel et al. [28] demonstrated variable detection ranges in an estuarine system were largely affected by water speed with complex tidal patterns. In Mathies et al. [31] – in the marine environment – sample size was small (two receivers and two tags = max four receiver-tag pairs) and strength of tidal effect variable, while other studies have included tidal height as a parameter [14] which may not necessarily capture the effect of water movement.

Here, we use a controlled telemetry investigation to quantify the influence of tidal cycle on the detection range and efficiency of acoustic receivers in a tidal system, to inform analysis of acoustic telemetry data in the area and design of a fine-scale acoustic telemetry array. Detection range and efficiency are modelled for a range of tag models and powers. We quantify the influence of tidal cycle on detection efficiency, accounting for the influence of other covariates including receiver tilt, background noise, and tidal height. We then explore the effect of tidal phase on detection range and efficiency across the whole tidal cycle, at slack water, and at mid-tide.

Methods

Study site and data collection

An acoustic telemetry array was set up around the Hinkley Point C nuclear powerplant sea water abstractions heads, located in Bridgwater Bay, the Bristol Channel, UK (Fig. 1). The area is a highly tidal environment – one of the largest tidal ranges in the world (tidal range of up to ~ 13 m in Bridgwater Bay during this study) – with a fine-mud seabed [32, 33]. Due to strong tidal currents, the environment is turbid and can have high suspended sediment concentrations [34].

During the study period, the array consisted of a total of 21 Innovasea (Halifax, Canada) receivers, of which six were VR2AR Acoustic Release receivers and 15 were VR2Tx Acoustic receivers (Fig. 1). All receivers operated on a 69 kHz frequency. The receivers were deployed within an area of 10.84 km^2. Note that not all receivers were deployed for the entire duration (Supplements Table S1). The VR2AR receivers were deployed on the seabed in an upright position with 75 kg of weight and attached to an acoustic release canister (RS Aqua ARC unit, Fig. 2D). Six VR2Tx receivers were deployed on the seabed attached to 50 kg of weight and fixed to be orientated upwards (Fig. 2F). The remaining 9 receivers were attached to permanent surface marker buoys pointing towards the seabed (Fig. 2C). All receivers, apart from the six VR2Tx receivers on the seabed, had internal sync tags programmed to emit a coded signal on a randomised 540–660 s burst interval, at either "low" ($n = 2$), "high" ($n = 8$), or "very high" ($n = 5$) power levels.

A total of 24 test tags were deployed in five distinct batches (of different numbers) to investigate detection range and probability (Fig. 1). Batches contained differing numbers of test tags and varied in start and end date and duration: test tag deployments are summarised in Supplements Table S2. Test tag models were either V9 ($n = 12$) or V7 ($n = 12$) and were chosen because of their use in long-term research on salmon (*Salmo salar*) smolts and twaite shad (*Alosa fallax*), two species of conservation interest at the Hinkley Point C site. All test tags were bottom-mounted. Four test tags in one batch were deployed on fishing line with floats meaning their location was mid-water column (4.4–4.7 m above the

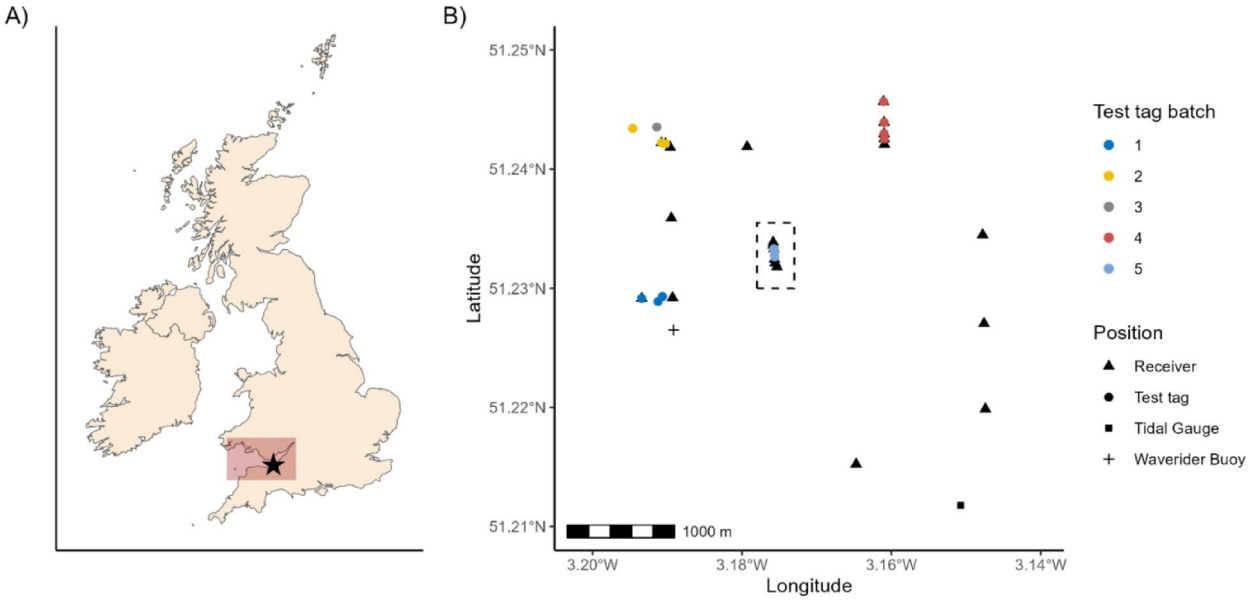

Fig. 1 Map of the study site, receivers and test tags and a diagram of receiver and test tag deployments. (**A**) Map of the UK and Ireland, with the Bristol Channel shown in red and the study location indicated by a black star. (**B**) Location of receivers and test tags included in this study as well as the Waverider buoy and tidal gauge which provided site-specific data on conditions and tide. The dashed-lines enclose the receivers and test tags that were deployed for a 10-day period in March 2025. Note that some receivers and test tags were co-deployed therefore overlap on the figure

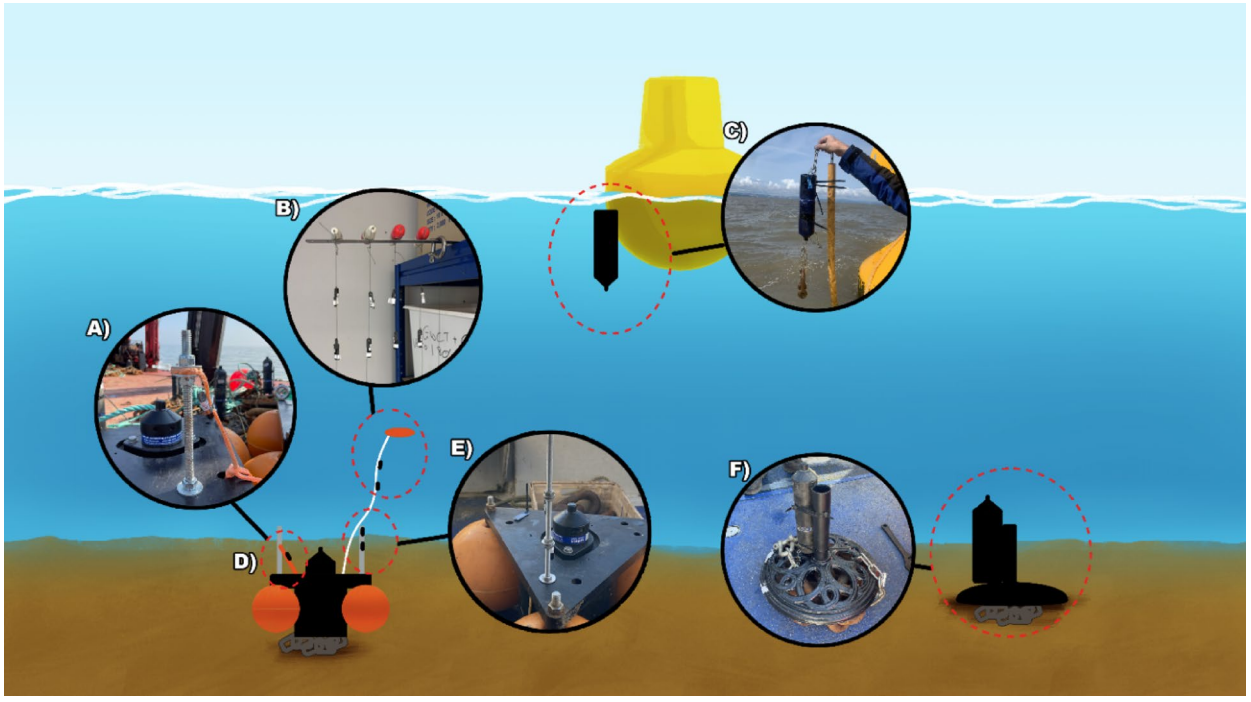

Fig. 2 Diagram showing the deployment of receivers and test tags. Test tags were either deployed with a receiver, attached to clump weights or attached to an umbrella stand (**F**). Test tags were attached via either a rope attached to a threaded bar (**A**), to a threaded bar itself (**E**) or midwater attached to fishing line and a float (**B**). Receivers were either deployed at the surface, attached to a surface marker buoy and orientated downwards (**C**), or bottom-deployed and orientated to the surface (**D** & **F**). Bottom-deployed receivers were either acoustic-release receivers (**D**) or attached to a clump weight (**F**) and were orientated upwards

mooring; Fig. 2B); the remaining test tag deployments were within 1 m of the mooring. Test tags had a random burst interval of 870–930 s and alternated between low and high-power level tag IDs (i.e. each tag ID was emitted on a randomised 1740–1860 s interval), meaning a total of 48 test tag IDs. Individual tags were deployed multiple times. Test tag ping rate selection may bias results depending on study duration with longer ping rates being inappropriate for short study durations. As test tags emitted a tag ID on ~30 min intervals, a brief exploration of the influence of tag burst interval is presented in the supplements which highlights that while with a short study duration a 30 min ping rate may be inappropriate, at high data quantities the issue is minimalised.

Test tag data were collected across different deployment periods from 14th August 2024 until 22nd April 2025. Receivers were recovered by 19th June 2025, meaning data on receiver sync tag detections were recorded until then. Distances between receivers and tags ranged from 0 to 4203 m (mean 1574 ± 1028 m standard deviation). A summary of receiver and test tag deployments and distances is provided in the supplementary materials in Tables S1, S2 and Figure S1.

Data processing

All data processing and analyses were conducted in R version 4.5.0 [35].

Prior to analysis, data were filtered to remove possible false detections and possible reflections. False detections are erroneous detections of a tag ID due to collisions of acoustic signals in the water. False detections generally occur isolated in time at a given receiver, i.e. they do not occur in bursts [36]. Detections were considered false detections and removed if they occurred > 24 h apart from another detection of that tag ID at a given receiver. Reflected detections occur when the transmitted signal bounces off a reflective surface (e.g. concrete wall, metal, etc.) before reaching a receiver. As a result, it is possible for a receiver to detect a given emission twice: once directly and again indirectly when reflected. To deal with possible signal reflections, we removed tag ID detections that occurred within the minimum burst interval (540 s for receiver sync tags, 1740 s for test tags) of its previous detection at a given receiver.

Hourly detection efficiencies were calculated for each receiver-tag pair, by calculating the ratio of detections recorded per hour to the number of pings expected. For each tag, the number of expected pings per hour was calculated for the nearest receiver that was deployed for the entire duration of that tag's deployment. Missing detections were identified via dividing the time between subsequent detections by the mean burst interval of the tag. To account for the random burst interval, the value was rounded to the nearest whole number: if the value was 2 or more, it indicated detections had been missed. Missing detections were then assigned a time stamp calculated as the mean burst interval from the previous detection. From here, the expected hourly number of pings per tag was determined and used to calculate detection efficiency per tag-receiver pair as a ratio of detected to expected pings. Due to the random nature of the burst intervals, sometimes a ping fell in the previous or following hour, resulting in a small amount of hourly detection efficiencies > 1 (~ 0.06% of total data). Since we could not be sure to which hour these pings belonged, we removed those few cases where hourly detection efficiencies were > 1.

Covariate data were assigned to each hour. Each receiver recorded hourly temperature and receiver tilt, as well as mean background noise: all receivers were subject to potential tilting. While receiver tilt and mean background noise were assigned to each hourly detection efficiency measurement without further manipulation, temperature records were summarised to a median hourly temperature to account for potential receiver recording errors and because temperature was not expected to vary significantly across the study site.

Tidal and wave data were obtained via a Waverider buoy (WaveNet data provided by Cefas on behalf of the data owner, EDF Energy https://wavenet.cefas.co.uk/details/HINKLY3DWR/INT) and tidal gauge present at the study site (Fig. 1C). Tidal height was recorded every 5 min by a downward-facing Valeport VRS20 Radar, connected to a Valeport Tidemaster, installed on the Hinkley Point C jetty: the data were also used to identify high and low tide times at the site. Tidal phase was defined as the data point's position in a 12 h tidal cycle between successive high tides. Given each data point spanned one hour, e.g. from 12:00:00 to 12:59:59, the time used was the middle of the hour, e.g. 12:30:00. As time between high waters during the study period varied between 12.2 and 13.2 h, values were corrected based on occurrence relative to high and low water times, such that 0 and 12 corresponded to high water and 6 to low water. The following wave data were recorded every 30 min: significant wave height (m), dominant peak wave period (s), average zero crossing wave period (s), and dominant peak wave direction (°). Tidal height and wave data were collated into hourly means. Wave data were unavailable from 00:00 on 30th April 2025 until 08:00 on 2nd May 2025 due to an issue with the buoy. Moon phase (range 0–1, where 0 = new moon, 0.5 = full moon, and 1 = new moon) was obtained via the `getMoonIllumination` function in the `sunCalc` R package [37].

Data were filtered to exclude data at times of receiver or tag deployment and receiver servicing or downloading. Finally, prior to analysis distances over 2 km, beyond which detections are unlikely, were removed to prevent zero-inflation [18].

Analysis

Overall detection ranges

We followed the same approach to calculate detection ranges as Edwards et al. [18], using dose-response curves via the R package `drc` [38]. As tag power is not comparable across tag models with regards to noise output, separate dose-response curves per tag power were made for test tag models and receiver sync tags with distance as an explanatory covariate. From the resulting curves, the distance at which detection efficiency was 50% (D50) and 5% (D05) were determined. D05 corresponds to what can be considered a maximum detection range and D50 is a midpoint range [39].

Effect of covariates on detection efficiency

Distances above the D05 for a given model were omitted from the second stage of analysis, as few detections are expected beyond that, as were distances of 0 m (e.g. co-located receiver-tag or a receiver's own sync tag) as detection efficiencies were high at this distance and may not provide much insight into environmental variability.

Covariate influence was investigated by comparing actual detection efficiency of a given tag-receiver combination to the predicted detection efficiency for that distance from the dose-response curves for each tag model [18]. Where actual detection efficiency was higher than predicted, a value of 1 was assigned; otherwise, 0 was assigned. The new binary response, representing improved or impaired detection efficiency, was then used as the response variable in a generalised additive mixed model (GAMM) using the R package `mgcv` [40].

As the response variable was already specific to a given tag model and power, and preliminary modelling indicated broadly similar patterns across tag models and powers, a single binomial GAMM was fitted to the data. Covariates investigated are listed in Table 1 and were transformed and explored before inclusion in the model. Receiver tilt was transformed into its sine, where 0° and 180° (i.e. vertical) both equal 1, while 90° (i.e. horizontal) equals 0, due to having both surface and bottom mounted receivers. For dominant peak wave direction, the cosine was used (0° and 360° = 1, 180° = -1). After these transformations, covariates were investigated for collinearity (Figure S3): none were deemed to be highly correlated (Supplementary materials), and all were included in saturated models (Table 1), though we note that several wave descriptors (average zero crossing wave period, dominant peak wave direction and dominant peak wave period) were moderately correlated (max 0.55) as were noise and the sine of receiver tilt (0.54). Continuous covariates were standardised prior to modelling, by subtracting the mean then dividing by the standard deviation.

The saturated model was, in `mgcv` format:

Improved efficiency ~ receiver depth * (temperature + tidal height + sin(receiver tilt) + noise + significant wave height + dominant peak wave period + cos(dominant peak wave direction) + average zero crossing wave period) + s(time since high water, bs = "cc", by=receiver depth, k = 12) + s(moon phase, bs= "cc", by=receiver depth, k = 12) + s(receiver_id, bs= "re").

where * denotes an interaction between receiver depth and all terms within the following brackets, s(…) represents the splines, "cc" indicates a cyclic cubic regression spline, k sets the basis dimension of the spline, and "re" means random effects. Moon phase and time since last high water were modelled as a cyclic cubic regression spline: all other covariates were linear. For test tags, the mooring height of the test tag (i.e. bottom versus midwater) was not included in models because on recovery it was discovered that tags were generally nearer to the bottom due to line-entanglements. The deployment depth of the detecting receiver (bottom versus surface) was included as an interaction with all covariates, to determine whether effects varied with deployment depth, considering all test tags were bottom-deployed and some covariates (e.g. surface wave parameters) may affect surface-deployed receivers more. Receiver ID was included as a random intercept in the model. Backwards stepwise model selection was applied using Akaike's Information Criterion (AIC) to compare models [41]. A more complex model was only retained if it reduced model AIC by at least 2 units. Smooths were not tested in model selection and instead interpreted based on model output. Fixed effects were visualised via predicting probabilities of improved detection across their ranges. Partial effects of the splines were extracted and plotted via the `gratia` package in R [42].

Tidal variation in detection range

To illustrate the impact of tides on detection range, dose-response curves were fitted to subsets of data for each hour of the cycle between high tides (i.e. the first twelfth, high water, being when time since last high water is < 0.5 h or > 11.5, the second twelfth being > 0.5 and < 1.5 etc.). D50 was calculated for each tag model for each tidal twelfth. Lastly, considering deployment of a fine-scale array at the study site, predicted efficiencies at 50, 100 and 150 and 200 m were extracted for the low-power V7s for slack water (tidal twelfth = 0 or 6) and mid-tide periods (tidal twelfth = 3 or 9) and compared to the overall values. The low-power V7 test tags were chosen as they were expected to have the lowest detection range of all test tags in the study, therefore providing a minimum expected detection range.

Table 1 Descriptions and summary statistics of covariates included in the statistical modelling of improved efficiency, defined as whether (or not) hourly detection efficiency was better than expected

Covariate	Description	Mean (± Standard deviation)	Median (Range)	Justification for inclusion + expectation
Receiver depth	Categorical covariate describing if the receiver was moored on the seabed (= bottom) or at a surface marker buoy (= surface)	–	–	Receivers moored at the surface may be affected more by surface waves while receivers moored at the bottom may be impacted more by suspended sediment.
Tidal height (m)	Tidal height at a given point in time relative to chart datum, provided via a gauge at Hinkley recording every 5 min.	6.30 (± 2.90)	6.20 (0.09–12.80)	Increased tidal height means increased water depth which affects detection efficiency. Higher detection efficiency is expected when water is deeper [29]
Corrected time since high water (h)	The time since the last high water, relative to the middle of each hourly bin, corrected for tidal cycle duration to be between 0 and 12	6.10 (± 3.50)	6.20 (0.08-12.00)	Increased water movement (such as tidal currents) lowers detection efficiency [25,26]. Tidal current will vary over the tidal cycle, expected to peak around 3 and 9 h after high water, and being lowest around 0, 6 and 12 h after the last high water. Detection efficiency is expected to peak when tidal current is expected to be lowest and vice versa.
Moon phase	Variable from 0 to 1 where 0 is a new moon and 0.5 is full moon	0.51 (± 0.28)	0.52 (0.001-1.000)	At new and full moons, tidal currents are greater, therefore it is possible that detection efficiency may be reduced at new and full moons.
Noise (mV)	Ambient noise, recorded by the VR2Tx and VR2AR receivers as an hourly mean	304.20 (± 125.00)	271 (5.00-944.00)	Detection efficiency is reduced when ambient noise is high [14,18].
Tilt (sine)	Tilt of the receiver, transformed into its sine for modelling	0.38 (± 0.27)	0.31 (0–1) NB. (0 = 0° or 180°; 1 = 90°)	A tilted receiver may be angled away from a tag and be unable to detect it [18,19].
Temperature (°C)	Ambient temperature recorded by receivers, median hourly value used in analysis	10.70 (± 3.90)	9.20 (5.70–20.30)	Detection efficiency increases as temperature increases, due to increased speed of sound in water [14].
Significant wave height (m)	Peak to trough height of the top third highest waves in each 30 min period.	0.48 (± 0.39)	0.37 (0.02–3.60)	Larger waves are expected to reduced detection probability [18].
Dominant peak wave period (s)	Represents the period associated with waves of significant wave height in each 30 min period	6.10 (± 3.50)	5.3 (1.70–24.00)	Greater wave period means bigger, more powerful waves and are expected to reduce detection probability.
Dominant peak wave direction (cosine)	Direction of approach of the waves contributing to significant wave heigh in each 30 min period. Transformed into its cosine for modelling	0.43 (± 0.32)	0.39 ((– 1.00)–(+ 1.00) NB. (-1 = 180°; 1 = 0° or 360°)	Waves from a more north-westerly direction at Hinkley Point C have a longer uninterrupted path and are expected to have a bigger effect on detection probability.
Average zero crossing wave period (s)	The average time duration between successive waves.	3.50 (± 0.97)	3.40 (1.80–8.50)	Wave period will affect wave size and power and air entrapment, while more frequent waves may also increase air entrapment [14].

Results

Overview on receivers and test tags

On recovery, four test tags (= 8 tag IDs) were found to be lost. While detections suggest the tags remained attached for at least one day, it is not known when they became detached from their mooring. As such, these tags were removed entirely from the data for the deployment on which they became lost (note that one of the tags had prior deployments where it contributed to the data, see Table S2).

The final data frame used in analyses was composed of 1,195,163 data points from 758 tag-receiver pairs, ranging 0 to 1998 m apart (mean 795 ± 673 m standard deviation). Excluding co-located receiver-tags, the distance apart ranged from 9 to 1998 m (mean 903 ± 646 m standard deviation). Of the data, 749,631 data points were for test tags and the remaining 445,532 for receiver tags. An overview of data is available in the supplements (Table S3).

Overall detection ranges

Detection ranges varied with tag type and power (Fig. 3; Table 2). D50s ranged from 88 m for the low power sync tags to 226 m for the high-power sync tags. Receiver sync tags generally had a higher D50s than the test tags, aside from the low power sync tags which had the lowest of all D50s. D50 increased as tag power increased, with the exception of the high and very high-power receiver sync

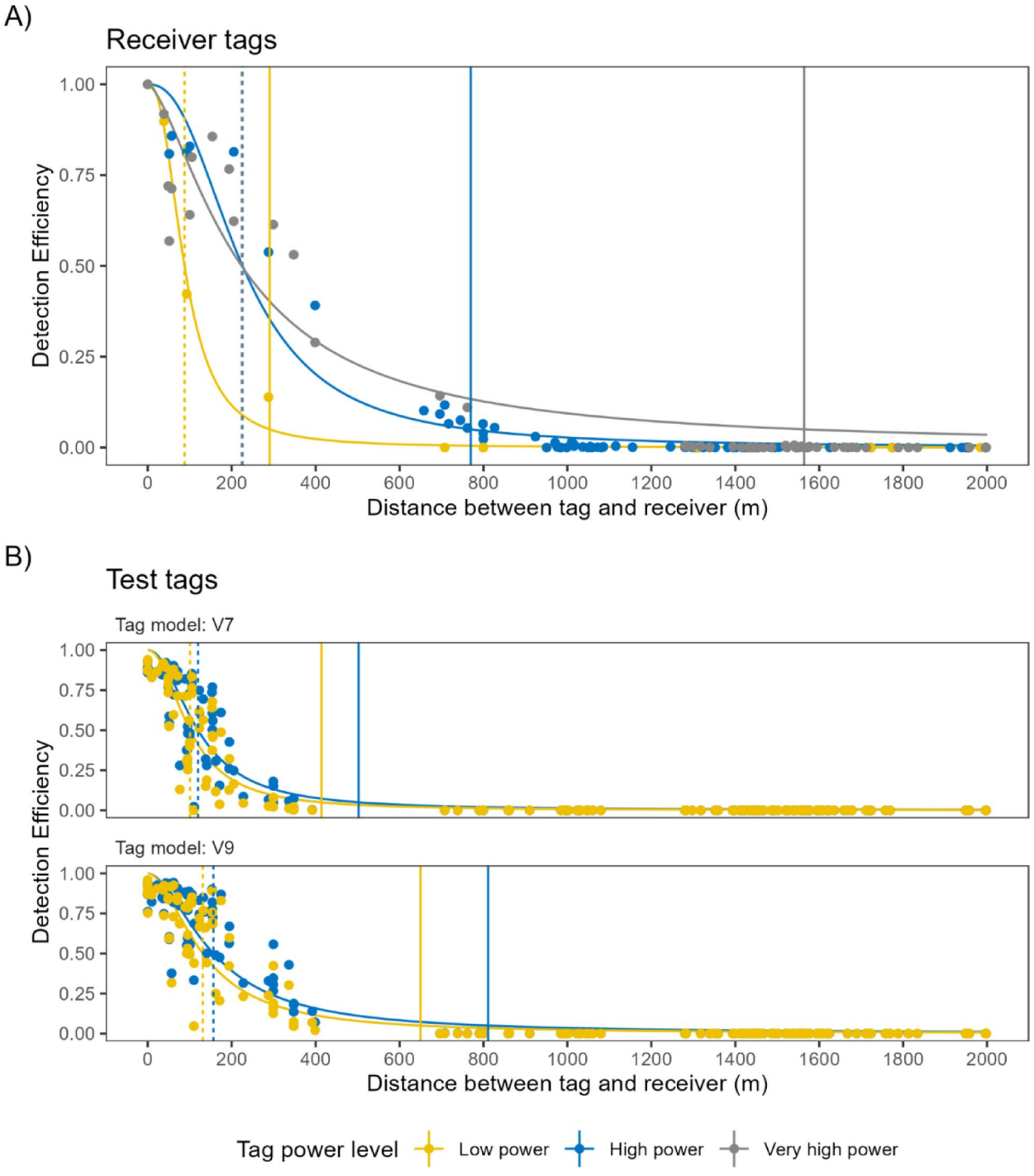

Fig. 3 Dose-response curves for (**A**) receiver sync tags and (**B**) the test tags. Dashed vertical lines show the distance at 50% efficiency while solid vertical lines show the distance at 5% efficiency. Points represent mean detection efficiencies for a given tag-receiver combination. Note in (**A**) the 50% detection efficiency dashed vertical line for high power tags is overlaid by that of very high power tags

tags, where the high-power tags had a greater D50 by ~ 2 m. In addition, the V9 test tags had a higher D50 than V7s for both power levels. D05s ranged from 290 m for the low power receiver tags to 1564 m for the very high-power receiver sync tags.

Influence of covariates on detection efficiency

The interaction between receiver depth and tidal height was removed in the AIC model selection: all other variables remained. Model coefficients and the AIC table is provided in the supplementary materials (Tables S4-6).

Table 2 Detection ranges from the dose-response curves for 50% detection efficiency (D50) and 5% detection efficiency (D05) across all tidal states. Detection ranges are given to the nearest whole number

Tag type	Tag power	D50 (m)	D05 (m)
Receiver sync tag	Low	88	290
	High	226	770
	Very high	224	1564
Test tag, V7	Low	101	414
	High	120	502
Test tag, V9	Low	131	650
	High	157	811

The tidal and lunar cycles affected detection efficiency (Fig. 4). Detection efficiency peaked around 6 and 12 h after the previous high water, i.e. slack water at low or high tide, with lowest detection probabilities around 3 and 9 h after high water, i.e. mid-tide where tidal velocity is expected to be greatest (Fig. 4A). Bottom-deployed receivers typically had a weaker relationship with tide, with a longer peak at low water and the high water peak occurring slightly early, while surface-deployed receivers experienced stronger tidal effects. In addition, there was asymmetry apparent: for surface deployed receivers, efficiency was lower for the outgoing tidal period (~3 h) compared to incoming (~9 h). For bottom-deployed receivers, the opposite was true though the difference was smaller. Moon phase also affected detection probability (Fig. 4B). Detection probabilities were highest around 0.3 and 0.8 (i.e. neap tides) while lowest around 0, 0.5 and 1 (i.e. spring tides). There was a prolonged trough around spring tides at 0.5. As with tidal cycle, the effects of moon phase were weaker for the bottom-deployed receivers.

Temperature, tidal height, average zero crossing wave period and dominant peak wave period had a positive effect on detection efficiency (Fig. 5). Receiver tilt, noise and significant wave height negatively affected detection efficiency (Fig. 5). The cosine of dominant peak wave direction had a positive effect on efficiency for bottom-deployed receivers (i.e. more northerly directions had improved efficiencies) and a negative effect for surface deployed receivers (i.e. more southerly directions had improved efficiencies): both effect sizes were small though (Table S4). The effect of tidal height did not vary with receiver depth. Surface-deployed receivers had stronger effects for: temperature, significant wave height, average zero crossing wave period and the cosine of dominant peak wave direction. The effect of significant wave height on surface-deployed receivers was the strongest of all variables. The effects of dominant peak wave period were similar in magnitude with receiver depth, but marginally greater for bottom-deployed receivers (coefficients 0.026 versus 0.024, Table S4). In addition, the effect of average zero crossing wave period on bottom deployed receivers was also comparatively weak, as with dominant peak wave period.

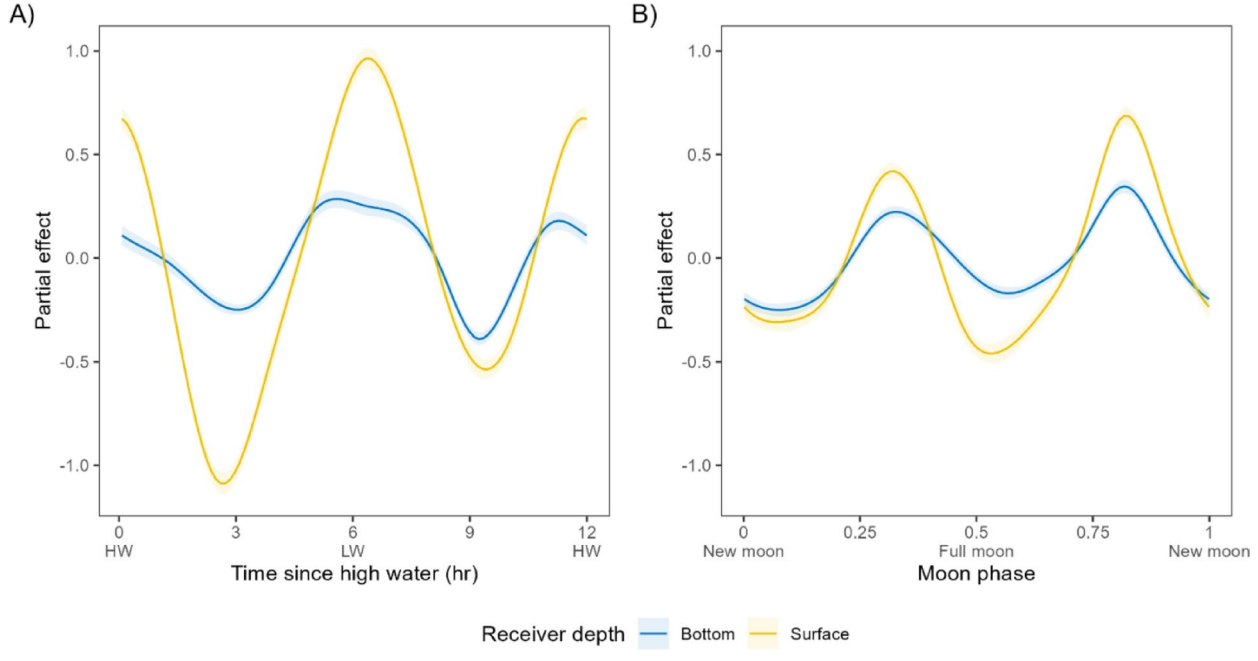

Fig. 4 Partial effects from a generalised additive mixed model, using cyclic cubic regression splines for time since high water (**A**) and moon phase (**B**). In Figure A, HW represents high water, and LW is low water. Receiver depth affected detection efficiency, with bottom-deployed receivers having a higher detection efficiency at a given distance compared to surface-deployed receivers. In addition, receiver mooring depth affected the strength of relationships with other covariates, with significant interactions between all terms excluding tidal height

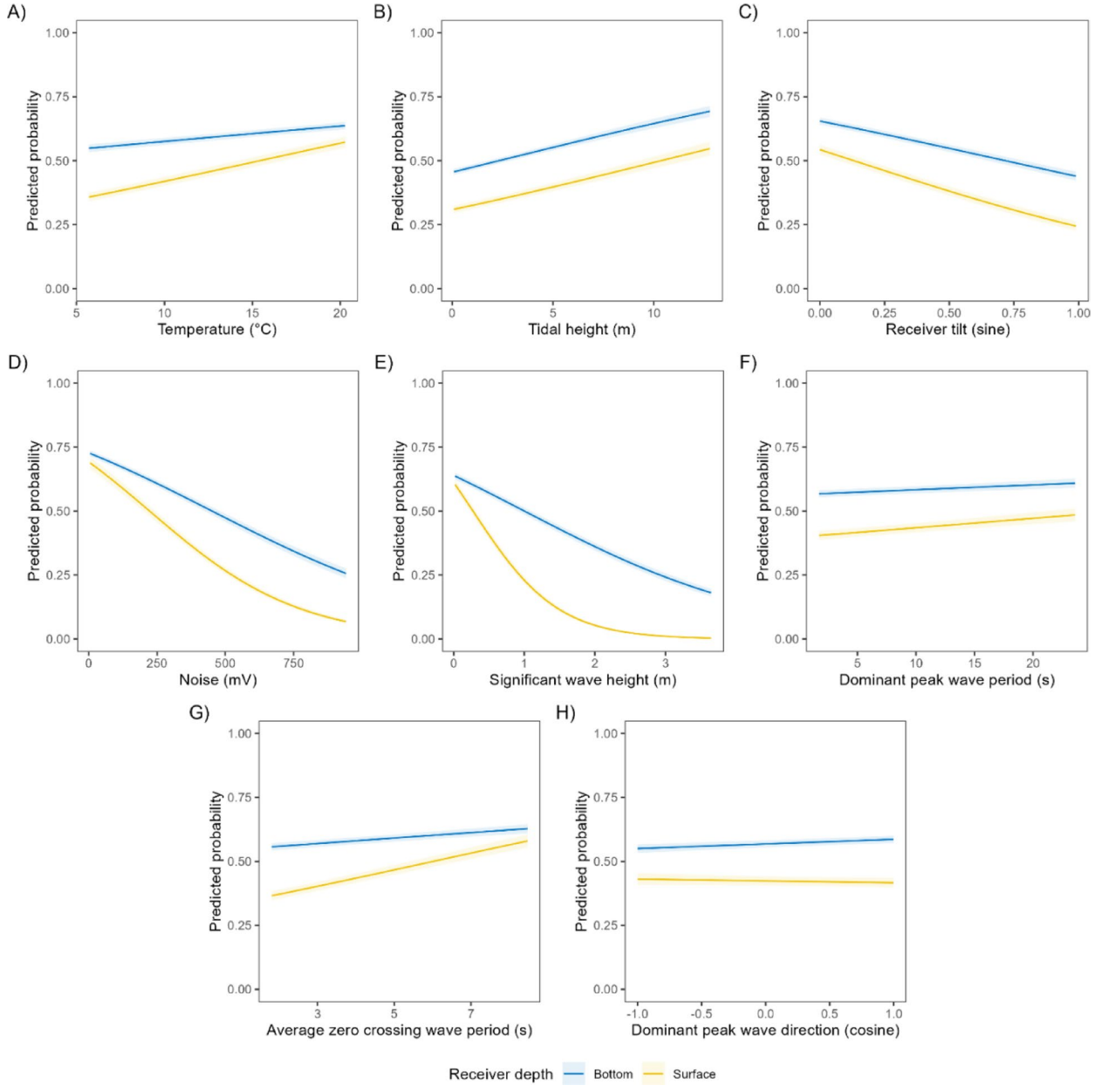

Fig. 5 Predicted probability of improved detection efficiency of acoustic telemetry tags with each covariate. The interaction between receiver depth and tidal height was not significant: in all other plots, the difference with receiver depth is considered significant. The 95% fixed-effect confidence intervals are shown. Plots show the change in predicted probability of improved efficiency with: (**A**) temperature; (**B**) tidal height; (**C**) sine of receiver tilt; (**D**) noise; (**E**) significant wave height; (**F**) dominant peak wave period; (**G**) average zero crossing wave period; and (**H**) cosine of dominant peak wave direction

Detection range in different tidal states

The D50 range fell during mid-tide periods (time since last high water = ~3 or ~9) and increased during slack waters (time since last high water = ~0, ~ 12 or ~6, Fig. 6). There was slight dissonance with the low water peak occurring around hour 7, i.e. one hour after low water. In addition, for the very high-power receiver tags, there was not an increase in D50 at high water, as observed with other tag types. Values at high water, low water and mid-tide periods for the low-power V7 test tags, low-power V9 test tags and high-power receiver tags are given in Table 3. The low-power V7 test tags are shown given they have the lowest detection range of all test tags while the high-power receiver tags have the most data of the receiver sync tags.

Considering the low-power V7 and high-power receiver sync tags in more detail, D50 increased to 305 and 367 m for the high-power receiver sync tags and to 137 and 115 m for the low-power V7 test tags at high and low waters, respectively. Mid-tide, D50 fell to 160 and

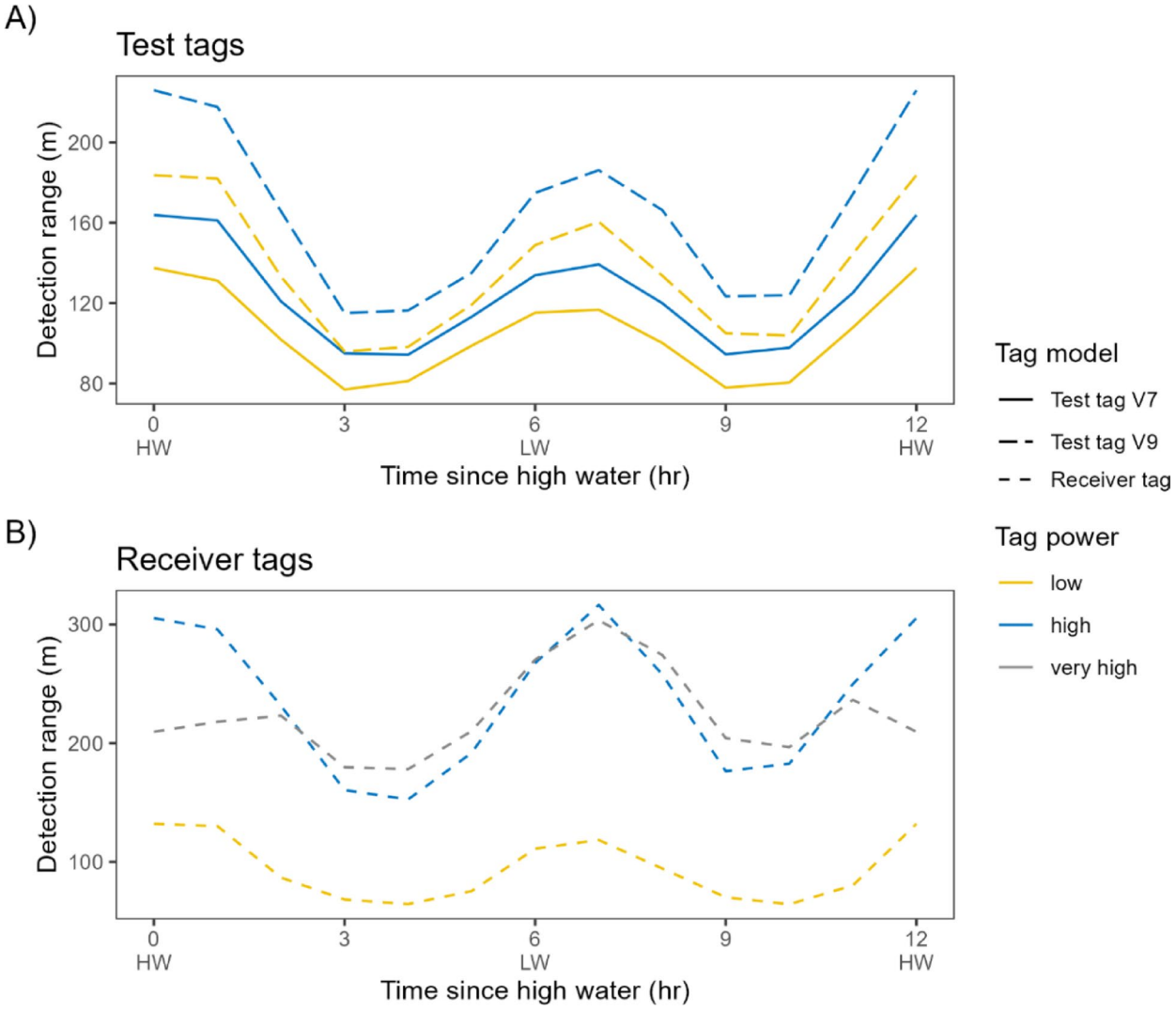

Fig. 6 Variation in the mid-point detection range (where detection efficiency is 50%) with tidal cycle for (**A**) test tags and (**B**) receiver sync tags across the tidal cycle. In the figure, HW refers to high water and LW to low water

Table 3 Predicted distances between receiver and tag for 50% detection efficiencies (D50) and 5% detection efficiencies (D05, considered maximum range) for high power receiver sync tags, low power V7 test tags and low power V9 test tags, at both slack waters and mid-tide periods. In the table, HW refers to high water (tidal twelfth = 0 or 12), LW refers to low water (tidal twelfth = 6), HW-LW is the mid-point of an outgoing tide (tidal twelfth = 3), and LW-HW the mid-point of an incoming tide (tidal twelfth = 9)

Tag type	D50 - distance with 50% detections efficiency (m)					D05 - distance with 5% detections efficiency (m)				
	Overall	HW	HW-LW	LW	LW-HW	Overall	HW	HW-LW	LW	LW-HW
Receiver sync tag, high power	226	305	160	367	176	770	1044	518	807	632
V7 test tag, low power	101	137	77	115	78	414	502	408	394	334
V9 test tag, low power	131	184	96	149	105	650	838	561	623	544

176 m for receivers and 77 and 78 m for test tags, representing a decrease of 56% and 44% from maximum to minimum values, respectively. By comparison, collating all data provided D50s of 226 m and 101 m respectively, representing a decrease of 66 m and 24 m mid-tide and an increase of 141 and 36 m at high water.

D05 – considered a maximum detection range – behaved similarly with tide for receiver tags, falling mid-tide and increasing at slack water. For the low-power V7s, D05 was at a maximum of 502 m at high water, with the high-low water period and low water having similar values (408 versus 394 m). It was lowest in the low-high water period (334 m).

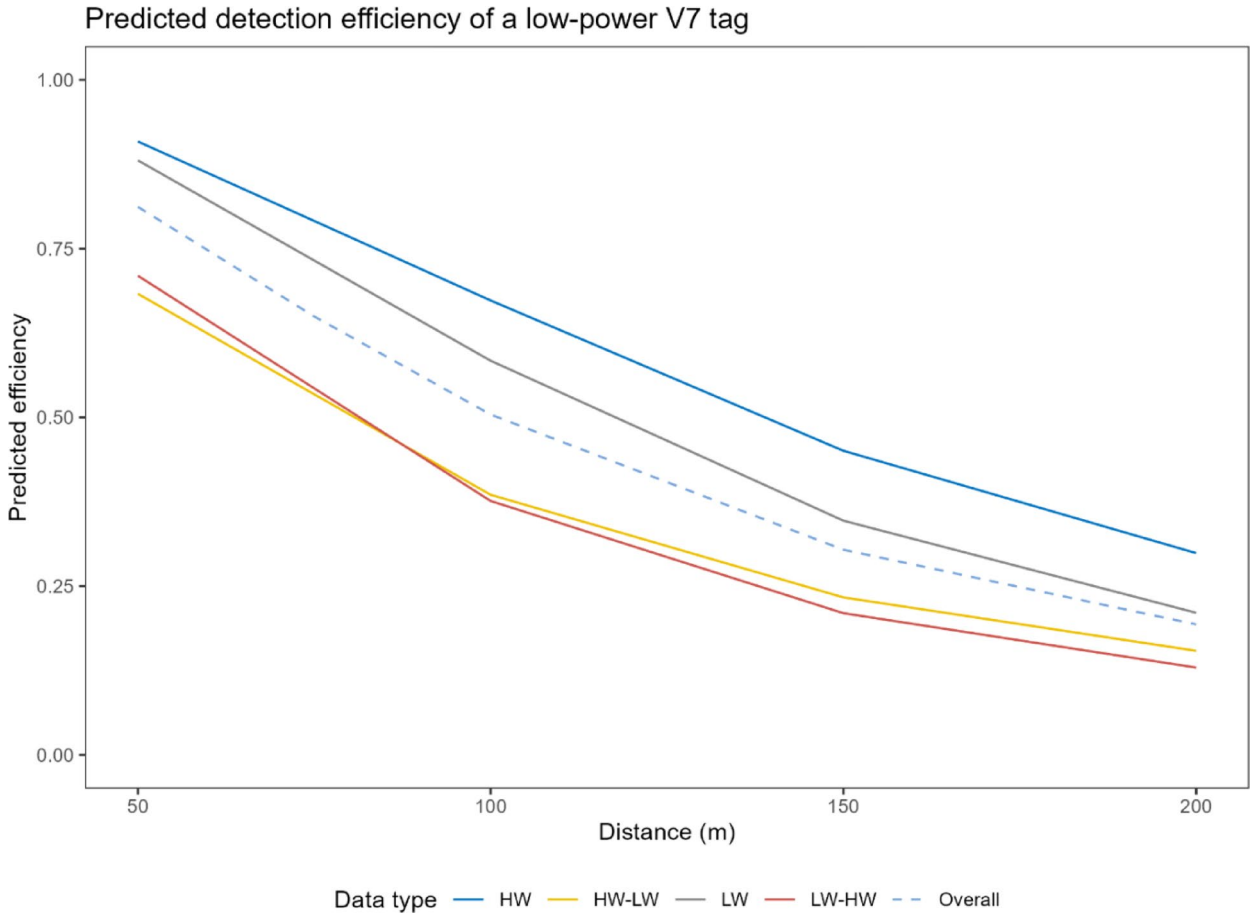

Fig. 7 Predicted detection efficiency for a low-power V7 tag at 50, 100, 150, and 200 m. Predicted efficiencies are shown for high water (HW, tidal twelfth = 0 or 12), low water (LW, tidal twelfth = 6), an outgoing tide (HW-LW, tidal twelfth = 3), an incoming tide (LW-HW, tidal twelfth = 9) and the overall values when considering all data together

Considering receiver spacing for a fine-scale array visited by animals tagged with low-power V7 tags, predicted efficiency at 50 m was 0.91 and 0.88 at high and low slack waters, and 0.68 and 0.71 for and the periods between high and low waters (Fig. 7). At the other extreme, efficiency at 200 m was 0.30 and 0.21 at high and low water while 0.15 and 0.13 during the mid-tide periods.

Discussion

Through analysing detection data from a variety of tag types and powers at surface and bottom-deployed receivers, we have described the influence of tidal cycle on detection range and efficiency in a tidal system. Detection efficiency and range are lowest between tides, when tidal currents are greatest with efficiency further decreasing at spring tides when tidal currents are stronger (compared to neap tides), suggesting a reduced ability to detect animals during these periods. As other variables such as tilt and noise were accounted for in our analyses and had low correlation with expected tidal currents, we propose that the remaining tidal variation represents water movement and associated effects (e.g. suspended sediment). With many telemetry studies set in coastal environments, understanding the influence of tide upon both detection efficiency and detection range is crucial to data interpretation.

Detection efficiency decreased between tides, when tidal current is greatest. Previously, tidal effects have largely been investigated in relation to tidal height [14, 29] or attributed to other mechanisms e.g. receiver tilt [18]. As receiver tilt and tidal height were accounted for separately in the GAMM, we suggest that the remaining observed variation in detection efficiency due to the tidal cycle represents the effect of tidal current on signal propagation. The negative impacts of water movement have previously been described [19, 25, 26], though effect sizes vary. Reubens et al. [19] noted minimal effects between the maximum and minimum current speed, though current speed in their study ranged from 0.13 to 0.92 ms^{-1}: at Hinkley, tidal current can reach ~ 1.7 ms^{-1} [43]. By comparison, water movement had the greatest impact in How and De Lestang [25], however we highlight "water

movement" in their manuscript encompasses not only current, but also movement due to swell etc. In addition, Merk et al. [26] found lower detection probabilities at higher current velocities in an estuarine system. Moreover, increasing sediment in the water column due to tidal current could further affect receiver performance by blocking signals [13, 25]. Detection efficiency was also reduced during spring tides – i.e. at full or new moon – during which tidal current is higher, supporting the idea that tidal current is the driver behind the changing efficiency. This finding differs somewhat from previous literature. How and De Lestang [25] investigated detection efficiencies in relation to the moon and found higher efficiencies at full moon, i.e. during spring tide. The differences between How and De Lestang [25] and our results may have emerged from several differences between the two studies. One notable difference between our study and How and De Lestang's [25] work is the way that moon phase was included in the models, where they included it as a linear term with 0 = new moon and 1 = full moon and we included it as a cyclic cubic spline. Looking ahead, using tidal phase as a covariate when modelling detection efficiency rather than tidal current itself might allow consideration of tidal current impacts in systems where tidal current data is not easily available (e.g. tidal current models are unavailable or behind a paywall, or researchers lack the ability to continuously measure tidal current during their study).

Implications for research are numerous. As tags are less likely to be detected mid-tide, this has major considerations for future studies of fish behaviour. Tide is a known cue affecting fish behaviour. For example, tidal phase has been linked to marine excursions by estuarine fish [44] while schooling behaviour has been linked to tides [45, 46]. For reef fish, increasing tidal current has been linked to reduced pelagic fish abundance, where fish take refuge from the flow [47]. As another example, fish activity has also been linked to tidal phase [48]. With this in mind, it is critical for acoustic telemetry users to be aware of tidal effects on receiver performance, lest inaccurate conclusions be drawn. Where detections decrease during mid-tide due to reduced detection efficiency, the erroneous interpretation of animal behaviour affected by tide could be drawn, such as for example animals leaving the study site or taking refuge in an area without a direct line of sight to receivers. Conversely, higher observed detections at slack water could be interpreted as increased presence. In reality, such observations could reflect variation in array performance, and, without corrections to the detection data, inferences from them could be spurious. For example, Payne et al. [23] accounted for detection variability by correcting the hourly number of cuttlefish detections by the mean detection frequency of control tags in that hour. Brownscombe et al. [39] presented an approach to account for and correct detection range variability over time. Both Brownscombe's et al. [39] and Payne et al.'s [23] approaches highlight the ability for researchers to correct for detection variability prior to analyses. Coastal acoustic telemetry users should determine detection efficiency and ranges under different tidal states, to understand the impact on their own research and then correct detections as needed. Deploying test tags as controls should therefore be considered, to enable corrections. Given test tag detection ranges vary with tag model and power, control test tags should therefore be of the same variety as tagged fish to permit accurate corrections. If researchers are unable to deploy test tags, caution should be taken when linking animal detections to the tidal cycle and perhaps aggregating data over a temporal scale coarser than the tidal cycle (e.g. daily presence) should be considered.

Understanding tidal effects on detection range and efficiency can also direct future study design, particularly fine-scale array design. For example, the observed tidal effects in this study influenced the subsequent deployment of a fine-scale array at Hinkley Point C, which will be used to monitor fish movements relatively to the infrastructure. Informed by preliminary analyses showing the lower mid-tide detection efficiency, the array was designed with a 50 m receiver spacing, with the intention of still having sufficient detections mid-tide for accurate positioning. With some fish tagged with low power V7s, the influence of tide on detection ranges and efficiency for the low power V7 test tags of the present analyses is particularly informative. Had we based the receivers spacing solely on the overall detection ranges from the present study (D50 = 101 m, D05 = 414 m) or on receiver spacing figures in literature (e.g. 150 m for a fine-scale array in the nearby English Channel [49] or Reubens et al. [19] in the North Sea reporting 70% detection efficiencies at ~ 200 m, although for different tag types), it is likely only few receivers would have detected any given ping at mid-tide resulting in a limited quantity and quality of subsequent animal positions. Indeed, mid-tide detection efficiency for the low-power V7s is ~ 0.7 at 50 m, falling to ~ 0.4 at 100 m, ~ 0.2 at 150 m and ~ 0.15 at 200 m, highlighting that even a 100 m receiver spacing – the overall D50 value – would have been inappropriate in this area. Without prior investigation into detection efficiency and range at the study site, our ability to study fish behaviour during tidal periods would have been compromised, limiting the ability to gain valuable conservation insight. Detection range studies typically quote a single value per study site and tag model for the duration of the study. Given we have demonstrated regular, predictable declines in detection range with tide – which may also vary predictably with other temporal patterns e.g. diurnally [23] – we postulate that during range testing,

researchers should calculate detection ranges across temporally-variable parameters e.g. slack water v mid-tide. By doing so, researchers can identify whether detection range regularly drops significantly and modify study design and analysis appropriately.

Of course, the impact of tide will likely vary with tidal strength. The Bristol Channel experiences one of the largest tidal ranges in the world [33] and tidal height at the study site during the study period ranged over 0–13 m. In other systems with weaker tides, effects may be reduced or even non-existent in locations with small tides. In Reubens et al. [19], tidal current range was small, limiting the overall effect of tidal current on detection efficiency. However, until more acoustic telemetry practitioners relate detection range and efficiency tests to tide, we cannot know the strength of effects in other systems. Moreover, we note that splines do not always completely adhere to an expect tidal or spring-neap cycle, e.g. peaks and troughs shifting slightly to when expected, prolonged troughs etc. This could be a byproduct of the splines themselves, where the number of basis functions meant a more complex shape could be fitted. A solution could be the application of harmonics in the model instead of splines, which have been used in other contexts to model temporally regular variability in data [50]. Alternatively, unique features of the site could contribute to this observation. For example, asymmetry was apparent for the effect of tidal cycle on detection efficiency. For surface-deployed receivers, the trough between high and low water – the ebb tide – exceeded that between low and high water – the flood tide. At Hinkley Point C, differing tidal current strength between ebb and flood tides have been reported, with a stronger ebb than flood tide observed during spring tides [43]; the difference between the tides decreases towards neaps. While the opposite was the case for bottom-deployed receivers, the difference was also weaker. Such variation could explain some of the patterns in the data, while other unknown idiosyncrasies with tide in Bridgwater Bay could explain further deviations from expected patterns.

Aside from tide, other covariates affected detection. Bigger, more frequent waves resulted in lower detection probabilities, likely due to waves producing noise and air-bubbles in the water. Air bubbles in water increase signal attenuation and scatter the sound signal, thereby reducing detections of tag transmissions [17, 51]. The negative effect of wave height has previously been described [29] and our findings echo the value of monitoring wave height. In Edwards et al. [18], the authors discussed the impact of wind speed and direction on detection efficiencies, linking wind's negative effects to wave action. Effect of dominant peak wave direction in our study was minimal and contrasting for surface vs. bottom-deployed receivers. The effect of wave direction could be more complex, and modelling direction as a cubic cyclic spline using degrees instead of cosine could enable more precise patterns e.g. specific angles with peak efficiency. Alternatively, additionally modelling the sine of wave direction could provide insight on east versus west effects of wave direction [18]. In addition, tidal height typically had a positive effect on detection efficiency, echoing previous studies. Long et al. [29] reported a similar effect of water depth, which had a similar range to our study, on their surface-deployed receivers. Similarly, Claisse et al. [52] reported increased detection range for deeper-deployed receivers (depth range 5–20 m). We note that tidal height is affected by time since high water (i.e. location in the tidal cycle) and, to a lesser extent, moon phase (i.e. more extreme values are expected at new and full moons) – both also being included in our model. We opted to still include tidal height in the model so that time since high water reflected the effect of tidal current on detection efficiency, and not the combined effect of tidal current and tidal height. The effect of tidal height is further emphasised by comparing detection across tidal states where, with the exception of high- and very high-power receiver tags, high water detection ranges were greater than low water values, indicating increased ability to detect fish at high water as a combination of low tidal current and increase water depth.

We also report negative effects of receiver tilt and noise, and a positive effect of temperature. Temperature typically has a positive effect on detection efficiency, as sound propagation in water increases with temperature [14, 18, 29]. The effects of noise and receiver tilt also agree with expectations and the literature. As ambient noise increases in the 69 kHz band, whether due to biotic (e.g. animal activity) or abiotic (e.g. wave action) factors, receivers are less likely to detect an acoustic transmission as the ambient sound can overpower transmissions. Meanwhile, as a receiver becomes more tilted, the antenna may no longer have a direct line-of-sight to a tag and a tag may fall in the receivers shadow, limiting detection efficiency [18], though we highlight that if a receiver is tilted in the direction of a tag, detection efficiency may be unaffected [19].

Receiver deployment depth affected detection probability. Bottom-deployed receivers generally had higher detection probabilities, particularly with test tags. Moreover, some of the covariates describing wave action (significant wave height and average zero-crossing wave period) had a weaker effect on bottom-deployed receivers. For surface-mounted receivers, wave action will likely have a larger effect for example due to increased noise or air bubbles interfering with signal transmission [19, 29]. Surface-deployed receivers were also more affected by tidal variables indicating that, in systems where a high tidal current velocity is expected, deploying receivers

on the seabed could improve detection probabilities and ranges. It must be noted that our results reflect that test tags were also mounted on the seabed, thus results indicate improved detection between tag and receiver when both are moored on the bottom, versus bottom to surface transmission with the surface-deployed receivers. If test tags had been successfully mounted mid-column – more representative of the behaviour of some fish species – the difference may have been less stark.

In this paper, we present the results of a GAMM, where the model indicates if a covariate improves detection efficiency compared to expected for that distance. As a result, models do not give a value for detection probability, rather the probability of improved efficiency. As such, we do not have a complete indication of effect size. We took this approach over a full integrated model (i.e. a GAMM that also includes distance as a covariate) due to computational reasons. In addition, predicted detection probabilities would be for specified conditions, e.g. the mean values of each covariate, and specific to those conditions. Covariates in our study varied greatly and some were uniformly distributed (e.g. time since high water and moon phase), meaning a predicted probability of detection may not actually be representative of the wider picture. As our main objective was to understand tidal influences on detection efficiency, rather than model exact probabilities, we consider our presented approach an acceptable option. Our paper takes a similar approach to Edwards et al. [18] while Huveneers et al. [22] modelled covariate effects on daily D50s. In addition, covariate influence may vary with distance. In Reubens et al. [19], noise and wind had little effect on detection efficiency at close distances, while as distance increased a negative effect emerges. Again, an interaction between distance and covariates was not included due to projected computational times and study objectives.

Here, we report detection ranges for several tag models and powers. Our ranges sit within published literature. The D50s in our study are similar to Edward et al. [18], who reported low and high power D50s of 123 and 149 m respectively in the Wadden Sea. The test tags in their study were V13s – a larger tag model with a higher output than the V7s and V9s used here – though our values for the V9 tags are moderately higher, highlighting site-specific differences and emphasising the need for range testing at each study site. Edwards et al. [18] also reported D50 for very high-power receiver sync tags of 311 m, far higher than reported in our study. In the wider detection range literature, detection ranges are variable and generally specific to a given study site due to for example topography or sediment [19, 25]. For example, Reubens et al. [19] reported detection probabilities of 0.7 up to 200 m in the Belgian North Sea, and noted their results are from winter months where harsher weather may reduce detection range. Meanwhile Huveneers et al. [22] reported a D50 of ~ 650 m off the Australian coast – more than triple the highest value in our study. To the other extreme, recent work by Kanno et al. [16] demonstrated 50% of detections were heard up to 20 m within a mangrove forest, versus up to 120 m outside, further emphasising the great variability with site-specific contexts. In How and De Lestang [25], D50s differed with both tag model and deployed site, ranging from 65 to 514 m across the south-west Australian coast, demonstrating inter-site variation and the need for study-specific range testing. Our variable detection ranges with tag type and power echoes Kessel et al.'s [14] earlier sentiment that detection range testing should include all tag types deployed during the study, or at least the tags with the lowest expected output (in our case, the low power V7s) for an idea of minimum detection ranges for tagged animals. Given the link between tag size (and power) and detection range, if animals are tagged with larger or smaller tags than used in this study, we expect different detection ranges from our results. Moreover, given the lower detection ranges for test tags (i.e. the tags used for animals) compared to receiver sync tags, it highlights a need to include test tags in detection range studies and not solely rely on the in-built receiver sync tags.

Compared to other detection range studies, our study contained a large number of receivers and test tags, and data collected over a long-time frame. We had 21 receivers deployed and 24 test tags, providing 758 receiver-tag combinations from 0 to 1998 m apart. By comparison, Reubens et al. [19] had seven acoustic receivers in their study resulting in 49 distances and no test tags. In addition, one of the few studies to consider tidal cycle, Mathies et al. [31], had just two receivers and two test tags, while Bruneel et al. [28] had eight receivers with in-built sync tags. Given the existence of inter-receiver variability in detections [28], and receiver ID widely treated as a random effect in models (e.g. Kanno et al. [16]), more tag-receiver combinations will strengthen conclusions. Moreover, our study covers ~ 10 months total for receiver sync tags and ~ 8 months for test tags, both including the winter months. Detection range can vary seasonally [24] and with short-term environmental conditions e.g. weather. Therefore, it is important for detection range studies to be conducted over a longer time frame covering poor or, ideally, different weather conditions. Reubens et al. [19] noted this – while their study lasted 22 days, it occurred during winter months when weather was harsher, thus they could presume that at other times with better conditions (e.g. summer) detection range may be increased. In How and De Lestang [25], one of their test periods at a specific site lasted seven days and had a drastically lower D50 than another site where the trial lasted 56 days: the poor performance

of the seven-day trial could represent a period of poorer conditions. We did not investigate seasonal variation in detection efficiency or range here. Moreover, we did not include weather covariates, which in turn may be linked to seasonal variability. For example, wave height and direction will be linked to wind speed [18, 19], with wind speed and direction influencing wave height and direction. On seasonal effects, it is possible that, during periods of harsher weather causing greater waves, mid-tide detection ranges and efficiencies will be even lower than reported here.

The test tags models used in this study – V7 and V9 tags – match those used in telemetry studies of two species of conservation concern in the Hinkley Point C study area, salmon smolts and twaite shad. The test tags alternated between a low- and high- power emission, with a given tag ID emitted roughly every ~ 30 min. In this study, hourly detection efficiencies were the basis of the analysis, meaning for the test tags one ping being missed by chance may potentially have an overwhelmingly large effect (e.g. if two pings were expected but one was missed due to chance, rather than due to environmental conditions, the efficiency is 0.5). However, taking a coarser detection efficiency window was not compatible with study goals. As the main focus of this research was tidal effects, a coarser window (e.g. 2–3 h) would have encompassed a much wider range of tidal current velocities, potentially dampening observed effects. We highlight that the study contained many test tags and receivers deployed over months, providing a greater volume of data than other studies (e.g. [19, 28, 31]). meaning the effect of a ping missed due to chance (rather than environmental conditions or distance), may have less of a bearing across the dataset (as supported by the analysis in the supplementary materials). While the study demonstrates the importance of tidal cycle on detection efficiency, the size of tidal effects presented in our GAMMs may be lower compared to if a faster ping rate was used (see supplementary materials). As a result, we emphasise the observed trends and relative effect sizes between receiver depth, rather than the absolute values from the GAMM,

Conclusion

Acoustic telemetry performance varies predictably with tidal cycle, with detection range and efficiency falling during mid-tide periods. Reduced mid-tide performance could lead to erroneous data interpretation regarding animal behaviour and limit the ability to position animals in fine-scale arrays. In addition, detection ranges differed with tag type and power. Our work highlights the value of calculating detection ranges across a regular temporally changing variable, e.g. tidal cycle, and conducting range testing using tags equivalent to animal tags in their study site.

Supplementary Information

The online version contains supplementary material available at https://doi.org/10.1186/s40317-026-00453-5.

Supplementary Material 1

Acknowledgements

We would like to think Dave Roberts and Paul Date for assistance with fieldwork. We would also like to acknowledge the funders of this work: Nuclear New Build Generation Company Ltd; Nature Networks Fund 3, Heritage Lottery and Welsh Government grant reference NM-23-01072; Welsh Government Tidal Lagoon Challenge; Natural England grant reference SRP027 - 10070036427; and Natural Resources Wales. Lastly, we would like to thank Luca Börger for feedback on an earlier version of the manuscript.

Author contributions

D.C., N.F. and R.V. secured initial funding for the project. D.C., G.B., O.D., A.J., T.L.-A. and C.R. were involved in conducting the deployment, recovery and maintenance of receivers and tags. M.B., D.M. and S.G. provided wave and tide data. R.M. conducted all data processing and statistical analysis. N.F., D.M. and S.G. provided feedback on the statistical analysis. R.M. wrote the main manuscript text. All authors provided feedback and revisions to the analysis and manuscript.

Funding

This research received funding from: Nuclear New Build Generation Company Ltd; Nature Networks Fund 3, Heritage Lottery and Welsh Government grant reference NM-23-01072; Welsh Government Tidal Lagoon Challenge; Natural England grant reference SRP027–10070036427; and Natural Resources Wales.

Data availability

The data used in this study are available from the corresponding author on reasonable request.

Declarations

Ethics approval and consent to participate

Not applicable.

Consent to publish

Not applicable.

Competing interests

The authors declare no competing interests.

Author details

[1]Department of Biosciences, Swansea University, Singleton Park, Swansea SA2 8PP, UK
[2]Centre for Environment, Fisheries and Aquaculture Science, Pakefield Road, Lowestoft, Suffolk NR33 0HT, UK
[3]Centre for Environment, Fisheries and Aquaculture Science, Barrack Road, Weymouth, Dorset DT4 8UB, UK
[4]Department of Life and Environmental Sciences, Faculty of Science and Technology, Bournemouth University, Poole BH12 5BB, UK
[5]Natural England, Met Office, Exeter EX1 3PB, UK

Received: 25 November 2025 / Accepted: 1 March 2026
Published online: 22 March 2026

References

1. Matley JK, Klinard NV, Barbosa Martins AP, Aarestrup K, Aspillaga E, Cooke SJ, et al. Global trends in aquatic animal tracking with acoustic telemetry. Trends Ecol Evol. 2022;37:79–94. https://doi.org/10.1016/J.TREE.2021.09.001.

2. Barnett A, Jaine FRA, Bierwagen SL, Lubitz N, Abrantes K, Heupel MR, et al. From little things big things grow: enhancement of an acoustic telemetry network to monitor broad-scale movements of marine species along Australia's east coast. Mov Ecol. 2024;12. https://doi.org/10.1186/s40462-024-00468-8.
3. Mawer R, Elings J, Bruneel SP, Pauwels IS, Pickholtz E, Pickholtz R, et al. Combining habitat selection, behavioural states, and individual variation to predict fish spatial usage near a barrier. Ecol Inf. 2025;85. https://doi.org/10.1016/j.ecoinf.2024.102967.
4. Vollset KW, Berhe S, Barlaup BT, Åtland Å, Isaksen TE, Wiers T, et al. High Level of Predation of Atlantic Salmon Smolt During Marine Migration. Marine Ecol. 2025;46(1):e12864 https://doi.org/10.1111/maec.12864.
5. Aspillaga E, Bruneel S, Alós J, Verhelst P, Abecasis D, Aarestrup K, et al. Open Protocols, the new standard for acoustic tracking: results from interoperability and performance tests in European waters. Anim Biotelemetry. 2024;12. https://doi.org/10.1186/s40317-024-00396-9.
6. Özgül A, Birnie-Gauvin K, Abecasis D, Alós J, Aarestrup K, Reubens J et al. Tracking aquatic animals for fisheries management in European waters. Fish Manag Ecol [Internet]. John Wiley and Sons Inc; 2024 [cited 2024 Nov 5];31. https://doi.org/10.1111/fme.12706
7. Lennox RJ, Aarestrup K, Alós J, Arlinghaus R, Aspillaga E, Bertram MG, et al. Positioning aquatic animals with acoustic transmitters. Methods Ecol Evol. 2023;2023:1–17. https://doi.org/10.1111/2041-210X.14191.
8. Matley JK, Klinard NV, Martins AB, Oakley-Cogan A, Huveneers C, Vandergoot CS, et al. TrackdAT, an acoustic telemetry metadata dataset to support aquatic animal tracking research. Sci Data Nat Res. 2024;11. https://doi.org/10.1038/s41597-024-02969-y.
9. Livernois MC, Ogburn MB, Legett HD, Richie KD, Aguilar R, Heggie K et al. Tracking animal movements via collaborative acoustic telemetry networks: Multiscale habitat use, phenology, and management insights. J Fish Biol. 2024; https://doi.org/10.1111/jfb.15952
10. Lubitz N, Butcher PA, Vianello P, Barnett A, Dwyer RG, Sheaves M, et al. Ocean warming increases residency at summering grounds for migrating bull sharks (Carcharhinus leucas). Sci Total Environ [Internet]. 2025;992:179966. https://doi.org/10.1016/j.scitotenv.2025.179966.
11. Piper AT, Manes C, Siniscalchi F, Marion A, Wright RM, Kemp PS. Response of seaward-migrating european eel (Anguilla anguilla) to manipulated flow fields. Proce R Soc B: Biol Sci. 2015;282:1–9. https://doi.org/10.1098/rspb.2015.1098
12. Armansin NC, Lee KA, Huveneers C, Harcourt RG. Integrating social network analysis and fine-scale positioning to characterize the associations of a benthic shark. Anim Behav Acad Press. 2016;115:245–58. https://doi.org/10.1016/j.anbehav.2016.02.014.
13. Orrell D, Webber D, Hussey N. A standardised framework for the design and application of fine-scale acoustic tracking studies in aquatic environments. Mar Ecol Prog Ser [Internet]. Inter-Research Sci Cent. 2023;706:125–51. https://doi.org/10.3354/meps14254.
14. Kessel ST, Cooke SJ, Heupel MR, Hussey NE, Simpfendorfer CA, Vagle S, et al. A review of detection range testing in aquatic passive acoustic telemetry studies. Rev Fish Biol Fish. 2014;199–218. https://doi.org/10.1007/s11160-013-9328-4.
15. Stott ND, Faust MD, Vandergoot CS, Miner JG. Acoustic telemetry detection probability and location accuracy in a freshwater wetland embayment. Anim Biotelemetry. 2021;9. https://doi.org/10.1186/s40317-021-00243-1.
16. Kanno S, Heupel MR, Hoel K, Schlaff A, Siddiqi A, Simpfendorfer CA. Performance and detection range of acoustic receivers in mangrove habitats. J Fish Biol. 2025;106:1540–53. https://doi.org/10.1111/jfb.15817.
17. Selby TH, Hart KM, Fujisaki I, Smith BJ, Pollock CJ, Hillis-Starr Z, et al. Can you hear me now? Range-testing a submerged passive acoustic receiver array in a Caribbean coral reef habitat. Ecol Evol. 2016;6:4823–35. https://doi.org/10.1002/ece3.2228.
18. Edwards JE, Buijse AD, Winter HV, Bijleveld AI. Gone with the wind: environmental variation influences detection efficiency in a coastal acoustic telemetry array. Anim Biotelemetry. 2024;12. https://doi.org/10.1186/s40317-024-00378-x.
19. Reubens J, Verhelst P, van der Knaap I, Deneudt K, Moens T, Hernandez F. Environmental factors influence the detection probability in acoustic telemetry in a marine environment: results from a new setup. Hydrobiologia. 2019;845:81–94. https://doi.org/10.1007/s10750-017-3478-7.
20. Gjelland KO, Hedger RD. Environmental influence on transmitter detection probability in biotelemetry: Developing a general model of acoustic transmission. Methods Ecol Evol. 2013;4:665–74. https://doi.org/10.1111/2041-210X.12057.
21. Singh L, Downey NJ, Roberts MJ, Webber DM, Smale MJ, van den Berg MA, et al. Design and calibration of an acoustic telemetry system subject to upwelling events. Afr J Mar Sci. 2009;31:355–64. https://doi.org/10.2989/AJMS.2009.31.3.8.996.
22. Huveneers C, Simpfendorfer CA, Kim S, Semmens JM, Hobday AJ, Pederson H, et al. The influence of environmental parameters on the performance and detection range of acoustic receivers. Methods Ecol Evol Br Ecol Soc. 2016;7:825–35. https://doi.org/10.1111/2041-210X.12520.
23. Payne NL, Gillanders BM, Webber DM, Semmens JM. Interpreting diel activity patterns from acoustic telemetry: The need for controls. Mar Ecol Prog Ser. 2010;419:295–301. https://doi.org/10.3354/meps08864.
24. Radigan WJ, Engel C, Chvala P, Longhenry C, Pegg M. Factors affecting detection probabilities of acoustic transmitters using passive receivers. Anim Biotelemetry. 2025;13. https://doi.org/10.1186/s40317-025-00411-7.
25. How JR, De Lestang S. Acoustic tracking: Issues affecting design, analysis and interpretation of data from movement studies. Mar Freshw Res. 2012;63:312–24. https://doi.org/10.1071/MF11194.
26. Merk B, Höhne L, Freese M, Marohn L, Hanel R, Pohlmann JD. To hear or not to hear: selective tidal stream transport can interfere with the detectability of migrating silver eels in a Tidal River. Anim Biotelemetry. 2023;11. https://doi.org/10.1186/s40317-023-00353-y.
27. Steel AE, Coates JH, Hearn AR, Klimley AP. Performance of an ultrasonic telemetry positioning system under varied environmental conditions. Anim Biotelem. 2014;2:1–17. https://doi.org/10.1186/2050-3385-2-15.
28. Bruneel S, Goossens J, Reubens J, Pauwels I, Moens T, Goethals P, et al. Turning the tide: understanding estuarine detection range variability via structural equation models. Anim Biotelemetry. 2023;11. https://doi.org/10.1186/s40317-023-00348-9.
29. Long M, Jordaan A, Castro-Santos T. Environmental factors influencing detection efficiency of an acoustic telemetry array and consequences for data interpretation. Anim Biotelemetry. 2023;11. https://doi.org/10.1186/s40317-023-00317-2.
30. Winter ER, Hindes AM, Lane S, Britton JR. Detection range and efficiency of acoustic telemetry receivers in a connected wetland system. Hydrobiologia. 2021;848:1825–36. https://doi.org/10.1007/s10750-021-04556-3.
31. Mathies NH, Ogburn MB, McFall G, Fangman S. Environmental interference factors affecting detection range in acoustic telemetry studies using fixed receiver arrays. Mar Ecol Prog Ser. 2014;495:27–38. https://doi.org/10.3354/meps10582.
32. Gao C, Adcock T. On the Tidal Resonance of the Bristol Channel. Int J Offshore Polar Eng. 2017;27:177–83. https://doi.org/10.17736/ijope.2017.as19.
33. Xia J, Falconer RA, Lin B. Impact of different tidal renewable energy projects on the hydrodynamic processes in the Severn Estuary, UK. Ocean Model (Oxf). 2010;32:86–104. https://doi.org/10.1016/j.ocemod.2009.11.002.
34. Manning AJ, Langston WJ, Jonas PJC. A review of sediment dynamics in the Severn Estuary: Influence of flocculation. Mar Pollut Bull. 2010;61:37–51. https://doi.org/10.1016/j.marpolbul.2009.12.012.
35. R Core Team. R: A Language and Environment for Statistical Computing [Internet]. Vienna, Austria: R Foundation for Statistical Computing; 2025. https://www.r-project.org/.
36. Simpfendorfer CA, Huveneers C, Steckenreuter A, Tattersall K, Hoenner X, Harcourt R, et al. Ghosts in the data: False detections in VEMCO pulse position modulation acoustic telemetry monitoring equipment. Anim Biotelemetry. 2015;3. https://doi.org/10.1186/s40317-015-0094-z.
37. Thieurmel B, Elmarhraoui A. suncalc: Compute Sun Position, Sunlight Phases, Moon Position and Lunar Phase. CRAN: Contributed Packages. 2022. https://doi.org/10.32614/CRAN.package.suncalc.
38. Ritz C, Baty F, Streibig JC, Gerhard D. Dose-Response Analysis Using R. PLoS ONE. 2015;10:e0146021. https://doi.org/10.1371/journal.pone.0146021.
39. Brownscombe JW, Griffin LP, Chapman JM, Morley D, Acosta A, Crossin GT, et al. A practical method to account for variation in detection range in acoustic telemetry arrays to accurately quantify the spatial ecology of aquatic animals. Methods Ecol Evol Br Ecol Soc. 2020;11:82–94. https://doi.org/10.1111/2041-210X.13322.
40. Wood SN. Generalized Additive Models: An Introduction with R. 2nd ed. Chapman & Hall; 2017.
41. Johnson JB, Omland KS. Model selection in ecology and evolution. Trends Ecol. Evol. Elsevier Ltd; 2004. pp. 101–8. https://doi.org/10.1016/j.tree.2003.10.013.

42. Simpson GL. gratia: An R package for exploring generalized additive models. J Open Source Softw. 2024;9:6962. https://doi.org/10.21105/joss.06962.
43. EDF. HPC PCSR3 – Sub-Chap. 2.1 – Site Description and Data [Internet]. 2017. https://www.edfenergy.com/sites/default/files/public_version_of_hpc_pcsr3_sub-chapter_2.1_-_site_description_and_data.pdf. Accessed 23 Sep 2025.
44. Murray TS, Cowley PD, Bennett RH, Childs A-R. Fish on the move: Connectivity of an estuary-dependent fishery species evaluated using 1 a large-scale acoustic telemetry array [Internet]. 2018. https://mc06.manuscriptcentral.com/cjfas-pubs
45. Capoccioni F, Leone C, Pulcini D, Cecchetti M, Rossi A, Ciccotti E. Fish movements and schooling behavior across the tidal channel in a Mediterranean coastal lagoon: An automated approach using acoustic imaging. Fish Res. 2019;219. https://doi.org/10.1016/j.fishres.2019.105318.
46. Embling CB, Sharples J, Armstrong E, Palmer MR, Scott BE. Fish behaviour in response to tidal variability and internal waves over a shelf sea bank. Prog Oceanogr. 2013;117:106–17. https://doi.org/10.1016/j.pocean.2013.06.013.
47. Eggertsen L, Hammar L, Gullström M. Effects of tidal current-induced flow on reef fish behaviour and function on a subtropical rocky reef. Mar Ecol Prog Ser Inter-Research. 2016;559:175–92. https://doi.org/10.3354/meps11918.
48. Brownscombe JW, Gutowsky LFG, Danylchuk AJ, Cooke SJ. Foraging behaviour and activity of a marine benthivorous fish estimated using tri-axial accelerometer biologgers. Mar Ecol Prog Ser Inter-Research. 2014;505:241–51. https://doi.org/10.3354/meps10786.
49. Stamp T, Pittman SJ, Holmes LA, Rees A, Ciotti BJ, Thatcher H, et al. Restorative function of offshore longline mussel farms with ecological benefits for commercial crustacean species. Sci Total Environ. 2024;951:174987. https://doi.org/10.1016/J.SCITOTENV.2024.174987.
50. Forrest SW, Pagendam D, Bode M, Drovandi C, Potts JR, Perry J et al. Predicting fine-scale distributions and emergent spatiotemporal patterns from temporally dynamic step selection simulations. Ecography. 2025;2025. https://doi.org/10.1111/ecog.07421
51. Zhu SJ, Ooi A, Skvortsov A, Manasseh R. Modelling underwater noise mitigation of a bubble curtain using a coupled-oscillator model. J Sound Vib Acad Press. 2023;567. https://doi.org/10.1016/j.jsv.2023.117903.
52. Claisse JT, Clark TB, Schumacher BD, McTee SA, Bushnell ME, Callan CK, et al. Conventional tagging and acoustic telemetry of a small surgeonfish, Zebrasoma flavescens, in a structurally complex coral reef environment. Environ Biol Fishes. 2011;91:185–201. https://doi.org/10.1007/s10641-011-9771-9.

Publisher's note